

The NIM Sr Optical Lattice Clock

Y Lin¹, Q Wang^{1,2}, Y Li^{1,2}, F Meng^{1,3}, B Lin^{1,2}, E Zang¹, Z Sun¹, F Fang¹, T Li¹
and Z Fang¹

¹Division of Time and Frequency, National Institute of Metrology, Beijing, 100029, China

²Department of Precision Instrument, Tsinghua University, Beijing 100084, China

³School of Electronics Engineering and Computer Science, Peking University, Beijing 100871, China

linyige@nim.ac.cn

Abstract. A ^{87}Sr optical lattice clock is built at the National Institute of Metrology (NIM) of China. The atoms undergo two stages of laser cooling before being loaded into a horizontal optical lattice at the magic wavelength of 813 nm. After being interrogated by a narrow linewidth 698 nm clock laser pulse, the normalized excitation rate is measured to get the frequency error, which is then used to lock the clock laser to the ultra-narrow $^1\text{S}_0$ - $^3\text{P}_0$ clock transition. The total systematic uncertainty of the clock is evaluated to be 2.3×10^{-16} , and the absolute frequency of the clock is measured to be 429 228 004 229 873.7(1.4) Hz with reference to the NIM5 cesium fountain.

1. Introduction

In recent years, the accuracy of optical clocks have surpassed the best cesium fountain clocks [1, 2, 3, 4]. There are extensive discussions on the future redefinition of the SI (International System of Units) second using optical atomic frequency standards [5, 6, 7]. Therefore, before the redefinition it is always desired to have more laboratories worldwide to research on optical clocks and make absolute frequency measurements independently to demonstrate their agreement and consistency. Here we report our work on building a ^{87}Sr optical lattice clock and its evaluation result.

2. Experimental setup

The experimental details of our Sr clock can be found in ref [8, 9, 10, 11], here a brief introduction is given. Figure 1 shows the schematic of our experimental setup. The Sr atom vapor coming out of an effusive oven is firstly collimated by a hot micro-channel nozzle and then enters a transverse cooling cube to be further collimated by 2-dimensional (2D) optical molasses. After that, the atomic beam passes through a 30 cm long spin-flip type Zeeman slower [8] and finally enters the magneto-optical trap (MOT) chamber. The viewport opposite to the Sr oven is extended ~ 50 cm away from the MOT chamber by a piece of vacuum tube and heated up to more than 110 °C to prevent it from the deposition of Sr atoms. The long vacuum tube ensures that the temperature increase of the MOT chamber induced by the heated window is insignificant and the solid angle of the heated window seen by the atoms is reduced.

Two stages of laser cooling are used to trap ^{87}Sr atoms. The first stage laser cooling is operated on the $^1\text{S}_0$ - $^1\text{P}_1$ transition at 461 nm with a natural linewidth of 32 MHz [8]. The 461 nm laser output is



divided into five beams, including absolute frequency lock, Zeeman slowing, 2D molasses cooling, MOT cooling and probe beams. All these five laser beams are frequency shifted by different acousto-optic modulators (AOMs) to meet specified frequency detuning requirements. These AOMs are also used as fast light switches in order to run the experiments according to a specified time sequence. At the same time, mechanical shutters are employed in the light paths to shut the light completely off. Two re-pump lasers at 679 nm and 707 nm are necessary for improving the cooling efficiency and for the transition probability measurement [9].

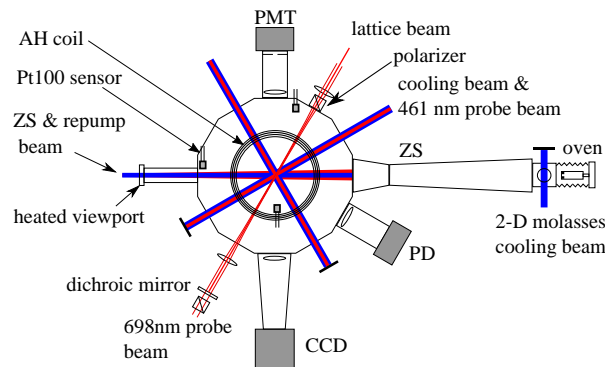


Figure 1. (color online) The schematic of the experimental setup. AH: anti-Helmholtz, ZS: Zeeman slower, PD: photodiode, PMT: photomultiplier tube

After the first stage laser cooling, the temperature of the atoms is ~ 3 mK. The atoms are then transferred to the second stage MOT utilizing the 1S_0 - 3P_1 transition at 689 nm with a natural linewidth of 7.5 kHz. The master laser for the second stage laser cooling is an external-cavity diode laser (ECDL). The frequency of this 689 nm ECDL is locked to a reference cavity (finesse $\sim 10,000$) installed in a temperature controlled vacuum chamber through Pound-Drever-Hall (PDH) method. The output of the master laser is amplified by two slave lasers, one with injection lock and the other with offset-frequency phase lock. The output of the two slave lasers are delivered to the MOT by two pieces of single mode polarization maintaining (SMPM) fiber. Two AOMs are used for broad-band frequency modulation of these two slave lasers to improve the transfer efficiency between the first stage and second stage MOT [9]. At the beginning of the transfer from the blue MOT to the red MOT, the 461 nm cooling laser is switched off and the 689 nm laser is switched on. The field gradient is rapidly dropped from 50 Gauss/cm to 3 Gauss/cm and then ramped up to 10 Gauss/cm in 100 ms. The 689 nm laser frequency is wideband modulated (deviation 3 MHz, modulation frequency 30 kHz) by the AOMs during the dropping down and the ramping up of the field gradient. The frequency modulation of the lasers are switched off at the end of the field ramp. After another 55 ms of narrow line laser cooling, the ^{87}Sr atoms can be cooled down to a temperature as low as 3 μK .

During the whole cooling process, the 813 nm lattice laser is switched on and overlapped with the atom cloud. The lattice laser is a commercial Ti: sapphire laser (Coherent MBR110 pumped by a Verdi-V10). The frequency of the lattice laser is locked to a homemade F-P cavity. During the evaluation and frequency measurement of the Sr clock, the absolute frequency of the lattice laser is measured by the optical frequency comb once per day. The lattice beam (~ 300 mW) is focused to the center of the MOT and then retro-reflected by a dichroic mirror to form a standing wave optical lattice. The dichroic mirror has high reflectivity at 813 nm and high transparency at 698 nm. The optical lattice is set to be horizontally oriented [9]. The lattice beam waist is ~ 42 μm and the trap depth is 29 μK . After the second stage laser cooling, more than 10^4 atoms are trapped and confined in the Lamb-Dicke regime in the longitudinal direction of the 1-dimensional optical lattice.

Our 698 nm master laser is an ECDL locked to a high finesse reference cavity with the PDH method to narrow its linewidth. Both the cavity spacer and the mirror substrates are made of ultra-low expansion (ULE) glass, which set the thermal noise limited stability to $\sim 1 \times 10^{-15}$ at 1 s [12]. The stability of our 698 nm laser is measured to be 3×10^{-15} @ 1 s from the beat note of two similar laser systems [10]. Since then, some modifications focusing on reducing the residual amplitude modulation noise of the electro-optic modulator have been made, and the stability of the laser has been further improved. The output of the master 698 nm ECDL is frequency shifted by a double-pass 240 MHz AOM and is used to injection lock an F-P laser diode to amplify its power. The AOM driven by a direct-digital synthesizer (DDS) is used to compensate the drift of the cavity and bridge the gap between the cavity mode and the clock transition frequency. At the MOT, the 698 nm light is precisely co-aligned with the 813 nm lattice laser from the opposite direction using the dichroic mirror mentioned above.

Rabi excitation is used to probe the 1S_0 - 3P_0 clock transition. A normalized technique for minimizing the effect of the shot to shot atom number fluctuation is used to measure the transition probability [9]. When the clock laser frequency is scanned over a span of more than 200 kHz, sideband resolved spectra of the clock transition are acquired, as shown in Figure 2. After the second stage laser cooling, the atoms are spin-polarized by being optically pumped to $|F=9/2, m_F=+9/2\rangle$ and $|F=9/2, m_F=-9/2\rangle$ stretched states alternatively using either σ^+ or σ^- polarization of the 689nm laser at $^1S_0(F=9/2)$ - $^3P_1(F=9/2)$ transition frequency [11]. The 698 nm probe laser is co-aligned with the lattice laser, and their polarizations are aligned with the bias magnetic field ($\sim 56 \mu\text{T}$), which is used to resolve the two stretched states. When atoms are optically pumped to a single spin sub-state, the Rabi transition linewidth can be as narrow as 3 Hz with a 698 nm probe pulse width of 320 ms, as shown in the inset of Figure 2. The actual atomic lock uses 80 ms probe pulse width (the Fourier-limited Rabi linewidth is ~ 10 Hz) to make the locking more reliable. Two independent digital servos are used to lock the clock laser time-multiplexed to the two stretched states. The average of the two digital locks, which takes 4 clock cycles, gives the center frequency of the Sr clock. A complete single clock cycle including two stages of laser cooling, spin polarizing, Rabi excitation and transition probability measurement takes 1018 ms.

3. Systematic shifts evaluation

Recently, the first systematic shifts evaluation of NIM's Sr clock has been made [13]. The evaluation of the systematic uncertainties is performed using the self-comparison method [14]. Two independent atomic servos that share the same physical apparatus are compared in a time-interleaved way. The systematic effects and their corrections with uncertainties are listed in Table 1.

Table 1. Frequency corrections and uncertainties of the Sr clock and of its absolute frequency measurement.

Contributor	Correction (10^{-16})	Uncertainty (10^{-16})
Lattice Stark	17.2	2.2
BBR Stark	49.7	0.7
2 nd order Zeeman	1.8	0.1
Density	12.0	0.3
Clock laser Stark	0	0.1
Line pulling	0	0.1
Sr total	80.7	2.3
statistical		13
Gravitational	-50.6	1.1
Fountain calibration		31
Fiber transfer	0	< 1
Measurement total		34

The dominant correction comes from the black-body radiation (BBR) induced frequency shift. The BBR shift and its correction factors have been studied in depth by many other groups [3, 15, 16]. In our clock, the ambient temperature is recorded continuously during the experiments. Three thin film PT100 sensing resistors are installed onto the MOT chamber. One is embedded in a screw hole in the stainless steel MOT chamber. The second one is stuck to the flange which connects the extended hot Zeeman slowing beam window and the MOT chamber. The last one is stuck to the top MOT window. During the frequency measurements, the temperature difference between these sensors is less than 0.3 °C, and the fluctuation of the temperature is less than 0.5 °C. The ambient temperature 22(1) °C gives the BBR shift correction $49.7(0.7) \times 10^{-16}$.

The second dominant frequency shift and uncertainty comes from the lattice AC Stark shift. In order to measure the “magic wavelength”, the lattice laser frequency is changed by locking to different modes of the reference cavity. At one lattice frequency, the lattice trap depth is modulated with a depth difference as large as 70 Er (Er is the lattice photon recoil energy) between two atomic servos to measure the shift sensitivity. Because the modulation of the lattice depth also changes the atomic density, the frequency shift caused by this atomic density change needs to be corrected. The zero shift frequency is determined to be 368 554 672(44) MHz. During the absolute frequency measurements, the lattice laser frequency is locked to the nearest cavity mode which is $\sim 370(3)$ MHz away from the zero shift frequency and measured by the optical frequency comb. The lattice trap depth during the measurements is 176(5) Er. The correction of the lattice AC Stark shift is $17.2(2.2) \times 10^{-16}$.

The density shift is measured with self-comparison method by alternating the atomic density. The density of the atoms trapped in the lattice is changed by applying different loading times from 200 ms to 800 ms in the first stage laser cooling. The stability of a typical differential measurement is shown (red squares) in Figure 3. Due to the high atom density and relatively high atom temperature (~ 4 μ K in the longitudinal direction of the lattice and ~ 10 μ K in the radial direction), we observed a large density dependent frequency shift. The correction for running the clock at high density is $12.0(0.3) \times 10^{-16}$.

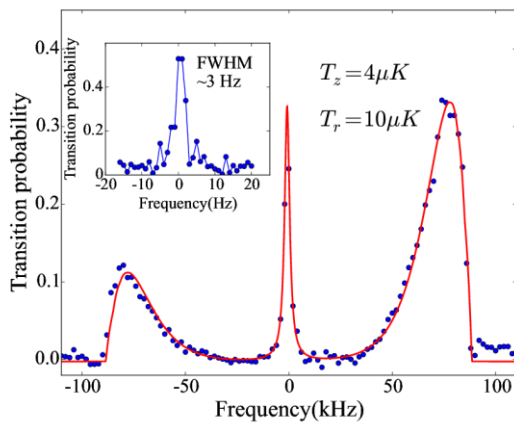


Figure 2. (color online) Sideband resolved spectra of the 1S_0 - 3P_0 transition. The red solid line is a fit to the experimental data, which gives the atoms' temperature. The inset is a high resolution spectrum (full width at half maximum ~ 3 Hz) of a single Zeeman component of the 1S_0 - 3P_0 transition with a Rabi excitation pulse width of 320 ms.

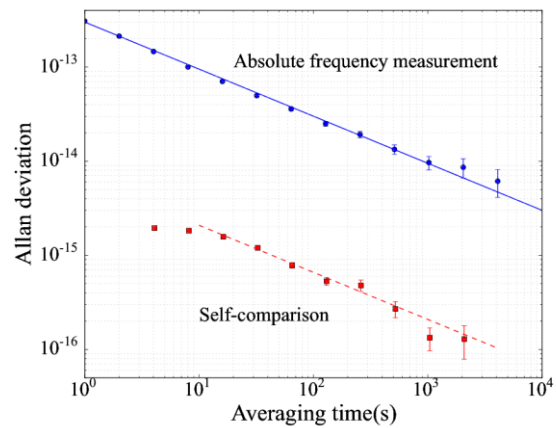


Figure 3. (color online) The measurement stability. The red solid squares show the Allan deviation (ADEV) of a typical self-comparison measurement of the density shift. The ADEV fits to (red dashed line) $6.6 \times 10^{-15} / \sqrt{\tau}$. The blue circles show the ADEV of a typical absolute frequency measurement which fits to (blue solid line) $3.0 \times 10^{-13} / \sqrt{\tau}$.

The clock laser is alternatively locked to the $m_F=+9/2$ and $m_F=-9/2$ components of the clock transition at a small bias magnetic field, and the first order Zeeman shift is canceled out when using the average of the two locks as the clock frequency. The frequency difference between these two locks gives the estimation of the magnetic field experienced by the atoms. With the coefficient in ref [2], the second order Zeeman shift is estimated to be $1.8(0.1) \times 10^{-16}$.

The clock laser power is several nW and the Stark shift caused by the clock laser is very small (less than 0.1×10^{-16}) using the coefficient value in ref [17]. With the transition linewidth of 10 Hz and the split between two adjacent m_F states of 62 Hz, less than 10% of atoms remain in the other states after spin-polarization contribute less than 0.1×10^{-16} uncertainty by line pulling effect. DC Stark shift may occur when electric charges trapped in the coating of the MOT chamber fused silica viewports [18]. The charges can be removed effectively by shining UV light on the viewports [18, 19]. An UV lamp is used to treat the viewports, and we found no significant shift. Other effects, that contributed very small shifts and uncertainties considering our present total uncertainty level, are omitted. The total systematic uncertainty of NIM's Sr clock is 2.3×10^{-16} .

4. Absolute frequency measurement

The system setup for the absolute frequency measurement is shown in Figure 4. In order to trace the absolute frequency of the NIM's Sr clock to NIM5 cesium fountain, the frequency of the flywheel H-Maser is delivered to the Sr laboratory (located at a different campus about 50 km apart) with a fiber noise cancellation system. The uncertainty introduced by the fiber transfer system is less than 1×10^{-16} [20]. The gravitational shift, according to Einstein's general theory of relativity, is calculated to be $50.6(1.1) \times 10^{-16}$ with the Sr clock altitude of 46.4 (1.0) m.

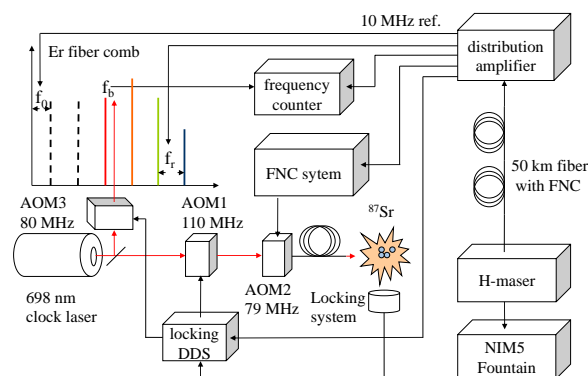


Figure 4. (color online) The schematic of the absolute frequency measurement. AOM: acousto-optic modulator. FNC: fiber noise cancellation.

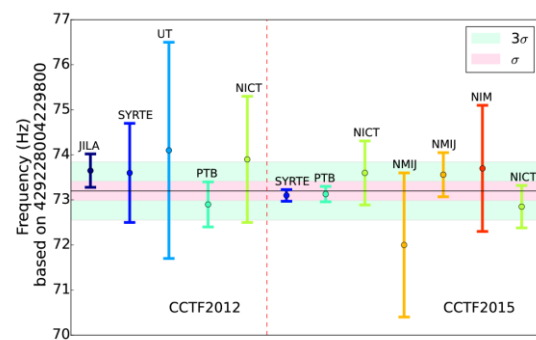


Figure 5. (color online) Sr clock frequency reported to CCL-CCTF FSWG. The black solid line is the 2015 recommended value. σ is the standard uncertainty of the recommended value.

A total of 49,113 s effective measurement data was acquired with 5 measurements. The Allan deviation of one of the measurements is shown (blue circles) in Figure 3. The statistical uncertainty of the total measurements is 1.3×10^{-15} . As shown in Table 1, the calibration uncertainty of NIM5 during the course of the measurements is 3.1×10^{-15} . The absolute frequency of the Sr clock is 429 228 004 229 873.7(1.4) Hz. This measurement result has been published in ref [13] and reported to the Consultative Committee for Length and the Consultative Committee for Time and Frequency Frequency Standards Working Group (CCL-CCTF FSWG) of the International Committee for Weights and Measures (CIPM) and agreed with the new recommended value of the Sr clock (shown in Figure 5 as black solid line), which is calculated by the weighted mean of all the effective measurements up-to-date [21, 22, 23, 24, 25, 26].

5. Conclusion

An optical lattice clock based on ^{87}Sr has been built and evaluated at NIM. The total systematic uncertainty of the clock is 2.3×10^{-16} . The absolute frequency of the clock has been traced to NIM5 cesium fountain with a measurement uncertainty of 3.4×10^{-15} . A new clock laser based on a long reference cavity is currently under development to further improve the stability of this Sr clock. We are planning to build the second Sr lattice clock in the near future.

6. Acknowledgment

The research is supported by the National Natural Science Foundation of China under Grant 91336212 and 91436104. The authors would like to thank W Chen, A Zhang, Y Gao and K Liang for their kind help.

References

- [1] Chou C, Hume D, Koelemeij J, Wineland D and Rosenband T 2010 *Phys. Rev. Lett.* **104** 070802
- [2] Bloom B, Nicholson T, Williams J, Campbell S, Bishof M, Zhang X, Zhang W, Bromley S and Ye J 2014 *Nature* **506** 71
- [3] Nicholson T *et al.* 2015 *Nat. Commun.* **6** 6896
- [4] Ushijima I, Takamoto M, Das M, Ohkubo T and Katori H 2015 *Nat. Photon.* **9** 185
- [5] Gill P 2011 *Phil. Trans. R. Soc. A* **369** 4109
- [6] Parker T 2012 *Review of Scientific Instruments* **83** 021102
- [7] Riehle F 2015 *arXiv:1501.02068*
- [8] Wang S, Wang Q, Lin Y, Wang M, Lin B, Zang E, Li T and Fang Z 2009 *Chin. Phys. Lett.* **26** 093202
- [9] Lin Y *et al.* 2013 *Chin. Phys. Lett.* **30** 014206
- [10] Li Y *et al.* 2014 *Chin. Phys. Lett.* **31** 024207
- [11] Wang Q, Lin Y, Li Y, Lin B, Meng F, Zang E, Li T and Fang Z 2014 *Chin. Phys. Lett.* **31** 123201
- [12] Numata K, Kemery A and Camp J 2004 *Phys. Rev. Lett.* **93** 250602
- [13] Lin Y *et al.* *Chin. Phys. Lett.* **32** 090601
- [14] Nicholson T, Martin M, Williams J, Bloom B, Bishof M, Swallows M, Campbell S and Ye J 2012 *Phys. Rev. Lett.* **109**
- [15] Yudin V, Taichenachev A, Okhapkin M, Bagayev S, Tamm C, Peik E, Huntemann N, Mehlstäubler T and Riehle F 2011 *Phys. Rev. Lett.* **107** 030801
- [16] Middelmann T, Falke S, Lisdat C and Sterr U 2012 *Phys. Rev. Lett.* **109** 263004
- [17] Baillard X, Fouché M, Le Targat, Westergaard P, Lecallier A, Le Coq, Rovera G, Bize S and Lemonde P 2007 *Opt. Lett.* **32** 1812
- [18] Lodewyck J, Zawada M, Lorini L, Gurov M and Lemonde P 2012 *IEEE Trans. Ultra. Freq. Cont.* **59** 411
- [19] Pollack S, Turner M, Schlamminger S, Hagedorn C and Gundlach J 2010 *Phys. Rev. D. Particles and fields* **81** 02110
- [20] Wang B, Gao C, Chen W, Miao J, Zhu X, Bai Y, Zhang J, Feng Y, Li T and Wang L 2012 *Scientific Reports* **2** 556
- [21] Campbell G *et al.* 2008 *Metrologia* **45** 539
- [22] Hong F *et al.* 2009 *Opt. Lett.* **34** 692
- [23] Yamaguchi A, Shiga N, Nagano S, Li Y, Ishijima H, Hachisu H, Kumagai M and Ido T 2012 *Appl. Phys. Express* **5** 022701
- [24] Le Targat *et al.* 2013 *Nat. Commun.* **4** 2109
- [25] Falke S *et al.* 2014 *New J. Phys.* **16** 073023
- [26] Akamatsu D, Inaba H, Hosaka K, Yasuda M, Onae A, Suzuyama T, Amemiya M and Hong F 2014 *Appl. Phys. Express* **7** 012401